International Journal of Offshore and Polar Engineering (ISSN 1053-5381)

Vol. 17, No. 4, December 2007, pp. 276–279

Residual Stress Evaluation for Weldment of Structural Components Using Instrumented Indentation Technique

Dongil Kwon*, Jung-Suk Lee and Jea-Hwan Han
Department of Materials Science and Engineering, Seoul National University, Seoul, Korea

Kwang-Ho Kim*
Frontics, Inc., Research Institute of Advanced Materials, Seoul National University, Seoul, Korea

Raghavan Ayer*, HyunWoo Jin* and Jayoung Koo*
ExxonMobil Research and Engineering Company, New Jersey, USA

We suggest a new instrumented indentation technique for estimating residual stress in weldments. This technique is based on the key concepts that the deviatoric stress part of the residual stress changes the indentation load-depth curve, and that through analysis of the difference between the residual stress-induced indentation curve and residual stress-free curve, the quantitative residual stress of the target region can be evaluated. To verify the applicability of the suggested technique, indentation tests and conventional tests were performed on natural gas pipeline weldments. The estimated residual stress values obtained using the indentation technique showed good agreement with those from conventional tests.

INTRODUCTION

Residual stresses caused by inhomogeneous thermal and mechanical loads during welding affect subsequent fracture and fatigue behaviour, stress-corrosion cracking and the like (Lu et al., 1996; Ruud et al., 1985). Thus the quantitative measurement of welding residual stress is important for the safe use and economical maintenance of industrial structures and facilities. Over the last few decades, a number of nondestructive methods has been developed, such as X-ray diffraction, the ultrasonic method, Barkhausen noise and neutron diffraction; these are based on the relationship between the physical or crystallographic parameters and the residual stress (Lu et al., 1996). Since the stress-sensitive parameters are, however, highly sensitive to metallurgical factors as well, applying these techniques to welded joints with rapid microstructural gradients is very difficult.

Thus an indentation technique, causing nearly nondestructive contact and being insensitive to environmental interferences, has been suggested for application in this research field (Sines and Carlson, 1952). However, the initial challenge was somewhat unsuccessful and pointless, because the alteration in hardness caused by the residual stress was less than 10% of its unstressed value. Recently, an instrumented indentation technique (IIT) that measures continuous deformation behaviour beneath an indenter as a curve of indentation load versus indenter penetration depth has been highlighted as an alternative to conventional mechanical tests (Doerner and Nix, 1986; Oliver and Pharr, 1992; Lee and Kwon, 1999; Ahn and Kwon, 2001; ISO—International Organization for Standardization—14577; KS—Korean Standards—B 0950). This technique has many advantages, such as good data reproducibility, feasibility for in-field applications, simplicity of testing procedure, and nondestructiveness. It has been used to evaluate various mechanical properties such as hardness, elastic modulus (Doerner and Nix, 1986; Oliver and Pharr, 1992), yield strength, tensile strength, work-hardening index (Ahn and Kwon, 2001) and fracture toughness (Lee and Kwon, 1999); analysis procedures for plastic stress-strain response and hardness are currently being standardized (ISO 1457; KS B 0950).

The stress sensitivity of the instrumented indentation curve and the application potential of this technique have been recognized by several researchers (LaFontaine et al., 1991; Zagrebelny and Carter, 1997).

However, most indentation studies for measuring stress have been tentative and somewhat empirical. Tsui et al. (1996) studied the influence of in-plane stress on indentation plasticity by investigating both the shape of the indentation curve and the remnant contact impressions. They reported that hardness was invariant regardless of the applied stress, and this was supported by subsequent finite element analysis (Bolshakov et al., 1996). Suresh and Giannakopoulos (1998) developed a theoretical model deriving a stress value from the ratio in the contact area of stressed and unstressed materials by separating out a plastic-deformation-related differential stress. However, hydrostatic stress still remained part of the differential contact stress, and the necessity of contact area observation for each indentation lessens the convenience of instrumented indentation. Thus, Lee and Kwon (2003) developed another instrumented indentation model that quantified the residual stress by analyzing the effect of surface stress on contact pressure in terms of shear plasticity. However, current theoretical models are difficult to apply to a general biaxial stress state because of their fundamental assumption of a simple equibiaxial stress state.

This study adapts Lee and Kwon's stress model to a general biaxial stress state and uses this model to characterize a friction stir-welded API X80 steel by suggesting proper assumptions for the stress directionality and reference stress-free information. The residual stresses estimated are compared with those from an energy-dispersive X-ray diffraction technique. In addition, the

*ISOPE Member.

Received June 9, 2007; revised manuscript received by the editors August 17, 2007. The original version (prior to the final revised manuscript) was presented at the 16th International Offshore and Polar Engineering Conference (ISOPE-2006), San Francisco, May 28–June 2, 2006.

KEY WORDS: Instrumented indentation, residual stress, friction stir welding, API X80 steel, stress directionality, energy dispersive X-ray diffraction.

influence of the characteristic microstructures in the friction stir-welded joint on local microhardness variation is discussed from a metallurgical viewpoint.

THEORETICAL MODEL

Model for Simple Surface Stress in Equibiaxial State

A surface residual stress is assumed to be in an equibiaxial tensile state ($\sigma_{res,x} = \sigma_{res,y} = \sigma_{res}$, $\sigma_{res,z} = 0$) and uniform in the near-surface region (taken as about 3 times the indentation depth) (Suresh and Giannakopoulos, 1998; Lee and Kwon, 2003). If an arbitrary indentation state (h_t, L_0) is attained in an unstressed state, and if the tensile in-plane stress σ_{res} is applied to the loading state at a fixed penetration depth h_t, the indentation load L_0 will be reduced to a smaller load L_T due to the decrease of surface penetration resistance. The load shift $L_T - L_0$ due to the application of tensile stress is a clue to stress quantification. The surface-normal deviator stress σ_Z^D is $-2\sigma_{res}/3$ (by removing the hydrostatic stress $-2\sigma_{res}/3$ from the surface residual stress σ_{res}) and is added to the contact pressure (Lee and Kwon, 2003). $L_T - L_0$ is assumed to be the product of the selected deviator stress component and its corresponding contact area A_C^T. Thus, an equation for the equibiaxial residual stress is derived in terms of the indentation load and contact area:

$$\sigma_{res} = 3(L_0 - L_T)/(2A_C^T) \tag{1}$$

Here A_C^T in the tensile stress state is calculated from $L_T \cdot A_C^T/L_0$ because the contact hardness **H** or $L_0/A_C^0 = L_T/A_C^T$ is independent of the elastic residual stress. In order to measure the actual contact area A_C^0 with pile-up or sink-in information from an Oliver–Pharr curve analysis (Oliver and Pharr, 1992), an empirical calibration for instrumental stiffness was performed through preliminary indentation tests on API X80 steel (Lee and Kwon, 2004).

Model Expansion for General Welding Stress in Biaxial State

Since the experiments and theoretical models described above treat only equibiaxial residual stress, the magnitude of the average stress effect can be determined with the instrumented indentation technique, but the directionality and magnitude of an actual biaxial stress cannot. This impedes wide application of the instrumented indentation technique to complex biaxial stress states in actual structures (Giannakopoulos, 2003). If we denote one major stress component of the biaxial residual stress $\sigma_{res,x}$ and the other as a minor stress component $\sigma_{res,x}$, $\sigma_{res,y}$ can be expressed as $\kappa\sigma_{res,x}$ using the stress ratio κ, i.e., $\sigma_{res,y}/\sigma_{res,x}$. The influence of biaxial stress on the indentation plasticity can also be analyzed through a similar hydrostatic stress removal method. The deformation-sensitive deviator stress component is given as $\sigma_Z^D = -(1+\kappa)\sigma_{res,x}/3$ in this case. Thus, if information on κ is given, individual principal stresses can be calculated from the instrumented indentation test using Eq. 2. Note that Eq. 2 converges to Eq. 1, when the stress state approaches the equibiaxial state or $\kappa = 1.0$.

$$\sigma_{res,x} = 3(L_0 - L_T)/((1+\kappa)A_C^T) \tag{2}$$

Lee and Kwon (2004) showed the validity of Eq. 2 by empirical indentation tests on biaxially strained specimens. The stress ratio became an important issue in stress characterization, and a nonsymmetrical contact deformation in uniaxial stress, observed by Underwood (1973), supplied a clue for extracting the surface stress directionality. Lee et al. (2004) tried to estimate the stress ratio by analyzing the pile-up heights along the 2 principal biaxial stress axes and found that the ratio of stress-induced pile-up shifts was linearly proportional to the stress ratio. Several preliminary observations on the welded joints yielded a stress ratio of about 0.33, and this value was used in subsequent biaxial stress analyses (Choi et al., 2005).

EXPERIMENTAL PROCEDURES

API X80 steel 20 mm in thickness was used in the friction stir-welding studies; its chemical composition (wt.%) is 0.13 C, 1.52 Mn, 0.26 Si, 0.17 Mo, 0.034 Cr, 0.026 Ni, 0.0002 Nb, 0.003 Ti, 0.062 V, 0.041 Al, 0.032 Cu, 0.0003 B. Test plates were sectioned in half along the rolling direction and prepared for a butt joint. Oxide scale was removed by sand grinding, followed by degreasing with methanol. An argon gas atmosphere was used to prevent oxidation during the weld cycle. Friction stir-welding was done with a polycrystalline cubic boron nitride tool in an inert gas environment (MegaStir Technology, West Bountiful, Utah, USA); tool rotation and travel speeds were 550 rpm and 1.69 mm s^{-1}, respectively. Metallographic samples for optical observation, Vickers microhardness, instrumented indentation testing (IIT), and energy-dispersive X-ray diffraction (ED-XRD) were prepared from the welded joint using metallographic procedures, followed by etching with a 2% nital solution. Vickers microhardness was probed using a 0.1 kgf load across the welded joint.

A commercial AIS 3000R (Frontics, Inc., Seoul, Korea) with depth and load resolutions of 0.1 μm and 14.7 mN was used for the instrumented indentation tests, which were performed across the friction stir-welded joint at 2-mm intervals. (A surface-parallel indentation testing array was made 2 mm from the welded surface.) Two methods were used to obtain a reference indentation curve in a stress-free state corresponding to each microstructural region in the welds. The reference stress-free curve for the base metal, which underwent no microstructural change, was obtained directly from the remote base-metal region (about 10 mm from the welds) (Lee et al., 2004). In addition, a multiple indentation method (5 kgf load gap) was applied to characterize contact properties at several depth steps. The reference stress-free curve for the welding zone, which underwent significant microstructural change, was calculated through a unique analysis (Lee and Kwon, 2004). The maximum applied load and testing speed were 50 kgf and 0.3 mm/min. We used ED-XRD with a high-energy white beam synchrotron radiation source. The profiling is done with the aid of highly collimated incident and scattered x-ray beams and with micropositioning of the sample surface. This stress profile obtained by ED-XRD was compared with that obtained by IIT.

RESULTS AND DISCUSSION

Microstructural Variation and Hardness Distribution in Welded Joint

Fig. 1 is a macro-image of the sectioned API X80 steel welds in which 4 distinctive microstructural regions can be identified from optical contrast differences; Fig.2 shows the corresponding microhardness variation. Whole microstructures in the welded joint had microhardness levels approximately similar to or above those of the base metal (BM), 180 to 210 kgf mm^{-2}. In particular, a region located near the advancing side in the thermomechanically affected zone (TMAZ) had microhardness above 300 kgf/mm^2. The presence of a hard zone (TMAZ-HZ in Fig. 2) and the gradual hardening behaviour from BM to TMAZ can be explained by

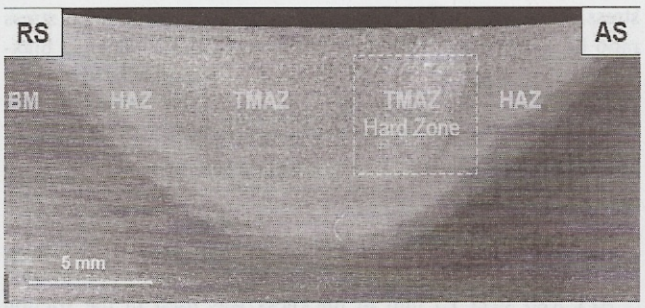

Fig. 1 Four distinctive microstructural regions within friction stir-welded API X80 steel

microstructural change. The microstructure of API X80 steel—the base metal in this study—is composed of ferrite, granular bainite and Martensite; its average grain size is 7 μm. The existence of fine ($\leq$100 nm) globular Nb,Ti(C,N) precipitates has also been reported by Bangaru et al. (2004). The microstructure of the heat-affected zone (HAZ) was nearly the same as that of the BM except for a slight grain refinement—the average HAZ grain size was about 5 μm. The microstructure of TMAZ was a mixture of granular bainite, degenerate upper bainite and lath Martensite; its grain was highly coarsened to about 15 μm. Although the average grain size increases over that in the BM and HAZ, the mixture of high-hardness phases increases the hardness of the TMAZ. The more dense acicular phases observed in the large TMAZ-HZ grain (about 30 μm) explain the significant hardness increment (Fig. 2).

Residual Stress Distributions Across Friction Stir-Welded Joint

The instrumented indentation curve of the BM near the HAZ (solid triangles) overlaps the API X80 steel reference indentation curve (Fig. 3). The load decrease due to surface stress at a given indentation depth means that the residual stress has positive sign (tensile). By inserting $\kappa = 0.33$ into Eq. 2, the quantitative stress distribution inside the base metal was calculated as plotted in Fig. 4. The BM reference indentation curve in Fig. 3 can be roughly fitted to $L = \alpha_B h^2$, where α_B is a hardness-proportional parameter. (About the upper 70% of the experimental solid line is fitted and overlapped in Fig. 3 as open triangles.) The approximate reference indentation curves for the HAZ, TMAZ and TMAZ-HZ also can be fitted by calculating corresponding α values. For example, α_{TMAZ} in the TMAZ is calculated from $\alpha_B H_{TMAZ}/H_B$. The hardness ratio of the TMAZ and BM H_{TMAZ}/H_B was about

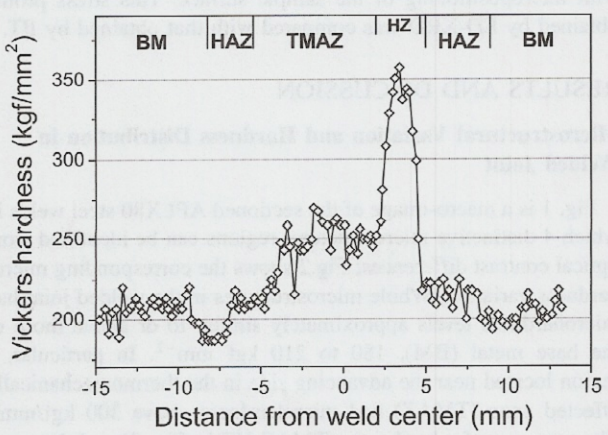

Fig. 2 Microhardness distribution across friction stir-welded joint

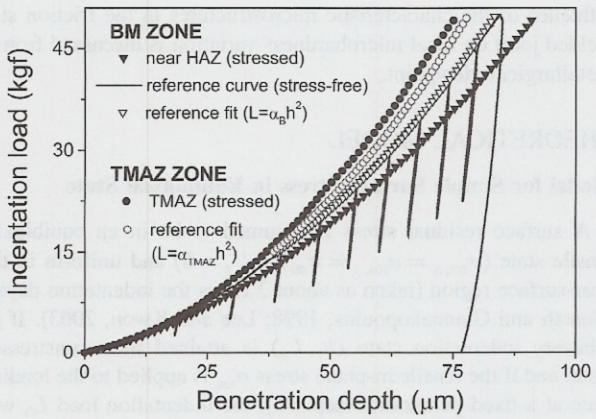

Fig. 3 Experimental indentation curves (solid triangles and circles) from welded joint in residual stress state and analytical reference curves (open triangles and circles) in stress-free state

1.21, thus α_{TMAZ} was 7.76×10^9 kgf m^{-2} when α_B for the BM was given as 6.41×10^9 kgf m^{-2}. The reference indentation curve calculated for the TMAZ-HZ is also plotted in Fig. 3 as open circles. Superposing the stressed indentation data and the newly calculated reference stress-free curve of the TMAZ (respectively, solid and open circles in Fig. 3) makes it possible to calculate a quantitative stress distribution in the TMAZ region. The stress distributions in the HAZ and TMAZ-HZ were also estimated by similar procedures.

Finally, the whole stress distribution in the friction stir-welded joint is plotted in Fig. 4 (solid circles). This figure also plots the residual stress profile measured from ED-XRD (open circles). Except for the slight negative shift of the ED-XRD results (less than 50 MPa), the residual stress distributions from IIT and ED-XRD were consistent throughout the whole welded joint. The discrepancy can be attributed to the indirectly calculated reference indentation curve and approximately determined stress ratio. The maximum tensile residual stress, about 150 MPa, was estimated near the BM-HAZ boundary, meaning that the BM-HAZ boundary is vulnerable to external loads. In addition, the high microhardness in the TMAZ-HZ region can be partially explained by the high compressive stress caused by the complex thermal cycle and phase transformation during the friction-stir welding.

These experimental results suggest that the instrumented indentation technique is a promising nondestructive stress-measurement method, especially for welded joints. However, the sparse indentation results, i.e. the 2-mm gap preventing the deformation field

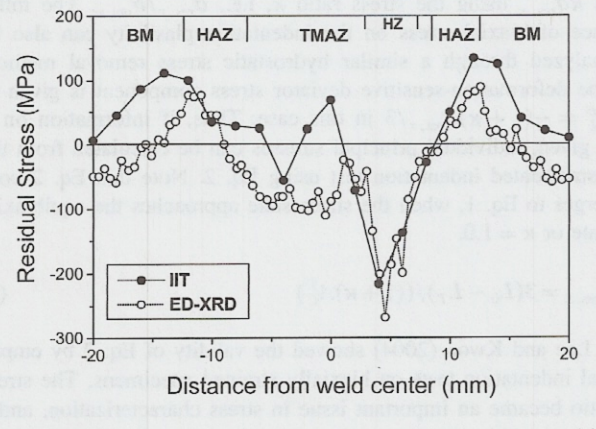

Fig. 4 Residual stress distributions measured by instrumented indentation technique (IIT) and energy-dispersive X-ray diffraction

overlap, should be improved for more local welds by adopting such indentation techniques as zigzag probing.

CONCLUSIONS

Local variations in microstructure, hardness and residual stress were explored using the microhardness and instrumented indentation techniques for friction stir-welded API X80 steel. Four distinctive microstructural regions were observed in the optically etched macro-image. Compared to the relatively fine grains (5 to 7 μm) in the heat-affected zone and base metal, the average grain sizes of the hard zone and its surrounding thermomechanically affected zone were large, about 30 and 15 μm, respectively. However, the microhardness in these microstructures showed a trend opposite the grain size, because the grains in the thermomechanically affected and hard zones contained dense, hard acicular phases. The residual stress profile assessed from the instrumented indentation technique showed high tensile stress (or compressive stress) near the base metal and heat-affected zone boundary (or near the thermomechanically affected zone–hard zone). Although there was a slight difference in quantitative value, the stress trend in instrumented indentation testing was perfectly consistent with the energy-dispersive X-ray diffraction results. Thus the instrumented indentation technique is a promising stress-measurement technique if its current limitations are handled successfully by reference indentation curve formation, stress ratio determination, and zigzag probing.

ACKNOWLEDGEMENT

The authors thank Prof. Thomas Tsakalakos at Rutgers University for the ED-XRD residual stress measurement.

REFERENCES

Ahn, JH, and Kwon, D (2001). "Derivation of Plastic Stress-Strain Relationship from Ball Indentation: Examination of Strain Definition and Pileup Effect," *J Mater Res*, Vol 16, pp 3170–3178.

Bangaru, NV, Fairchid, DP, Macia, ML, Koo, JY, and Ozekcin, A (2004). "Microstructural Aspects of High Strength Pipeline Girth Welds," *presented at 4th Int Conf Pipeline Tech*, Ostend, Belgium, 9–13 May.

Bolshakov, A, Oliver, WC, and Pharr, GM (1996). "Influences of Stress on the Measurement of Mechanical Properties Using Nanoindentation: Part II. Finite Element Simulations," *J Mater Res*, Vol 11, pp 760.

Choi, Y, Lee, YH, Jang, JI, Park, SK, Kim, KH, Seo, YW, and Kwon, D (2005). "Nondestructive Evaluation of Welding Residual Stress in Power Plant Facilities Using Instrumented Indentation Technique," *Key Eng Mater*, Vol 297–300, pp 2122–2127.

Doerner, MF, and Nix, WD (1986). "A Method for Interpreting the Data from Depth-Sensing Indentation Instruments," *J Mater Res*, Vol 1, pp 601–609.

Giannakopoulos, AE (2003). "The Influence of Initial Elastic Surface Stresses on Instrumented Sharp Indentation," *J Appl Mech*, Vol 70, pp 638–643.

ISO (International Organization for Standardization) 14577. HQs, Englewood, CO, USA.

KS (Korean Standards) B 0950, organization, Seoul, Korea.

LaFontaine, WR, Paszkiet, CA, Korhonen, MA, and Li, CY (1991). "Residual Stress Measurements of Thin Aluminum Metallizations by Continuous Indentation and X-ray Stress Measurement Techniques," *J Mater Res*, Vol 6, pp 2084.

Lee, YH, and Kwon, D (1999). "Evaluation of Fracture Toughness Through the Modeling of Indentation Residual Stress Field and Crack Shape," *Key Eng Mater*, Vol 569, pp 161–163.

Lee, YH, and Kwon, D (2003). "Measurement of Residual Stress Effect by Nanoindentation on Elastically Strained (100)W," *Scripta Mater*, Vol 49, pp 459–465.

Lee, YH, and Kwon, D (2004). "Estimation of Biaxial Surface Stress by Instrumented Indentation with Sharp Indenters," *Acta Mater*, Vol 52, pp 1555–1563.

Lee, YH, Kwon, D, Jang, JI, and Kim, WS (2004). "Residual Stress on Mechanical Indenting Deformation," *Key Eng Mater*, Vol 270–273, pp 35–40.

Lee, YH, Takashima, K, Higo, Y, and Kwon, D (2004). "Micromechanical Analysis on Residual Stress-Induced Nanoindentation Depth Shifts in DLC Films," *Scripta Mater*, Vol 51, pp 887–891.

Lu, J, James, MR, and Roy, G (1996). *Handbook of Measurement of Residual Stresses*, Fairmont Press, Inc., Lilburn, Georgia, USA.

Oliver, WC, and Pharr, GM (1992). "An Improved Technique for Determining Hardness and Elastic Modulus Using Load and Displacement Sensing Indentation Experiments," *J Mater Res*, Vol 7, pp 1564–1583.

Ruud, CO, DiMascio, PS, and Yavelak, JJ (1985). "Comparison of Three Residual-Stress Measurement Methods on a Mild Steel Bar," *Exp Mech*, Vol 25, pp 338–343.

Sines, G, and Carlson, R (1952). "Hardness Measurements for Determination of Residual Stress," *ASTM Bulletin*, Vol 180, pp 35.

Suresh, S, and Giannakopoulos, AE (1998). "A New Method for Estimating Residual Stress by Instrumented Sharp Indentation," *Acta Mater*, Vol 46, pp 5755–5767.

Tsui, TY, Oliver, WC, and Pharr, GM (1996). "Influences of Stress on the Measurement of Mechanical Properties Using Nanoindentation: Part I. Experimental Studies in an Aluminum Alloy," *J Mater Res*, Vol 11, pp 752–759.

Underwood, JH (1973). "Residual-Stress Measurement Using Surface Displacements Around an Indentation," *Exp Mech*, Vol 13, pp 373–380.

Zagrebelny, AV, and Carter, CB (1997). "Indentation of Strained Silicate-Glass Films on Alumina Substrate," *Scripta Mater*, Vol 37, pp 1869–1875.